

1 **The interprovincial green water flow in China and its tele-**
2 **connected effects on socio-economy**

3 Shan Sang^{1,2}, Yan Li^{1,2}, Chengcheng Hou^{1,2}, Shuangshuang Zi^{1,2}, Huiqing Lin^{1,2}

4 ¹State Key Laboratory of Earth Surface Processes and Resources Ecology, Beijing Normal
5 University, Beijing, China

6 ²Institute of Land Surface System and Sustainable Development, Faculty of Geographical Science,
7 Beijing Normal University, Beijing, China

8
9 **Corresponding Author:**

10 Yan Li, Ph.D.

11 Institute of Land Surface System and Sustainable Development, Faculty of Geographical Science,
12 Beijing Normal University, Beijing, 100875, China

13 Email: yanli.geo@gmail.com

14

15 **Abstract:** Green water (terrestrial evapotranspiration) flows from source regions,
16 precipitates downwind via moisture recycling, recharges water resources, and sustains
17 the socio-economy in sink regions. However, unlike blue water, there has been limited
18 assessment of green water flows and their tele-connected effects on socio-economy.
19 This study used a climatology mean moisture trajectory dataset produced by the Utrack
20 model for 2008-2017 to quantify interprovincial green water flows in China and their
21 socio-economic contributions. Results reveal an interconnected flow network where
22 green water of each province reciprocally exchanges with each other. Despite self-
23 recycling (ranging from 0.6% to 35%), green water mainly forms precipitation in
24 neighboring provinces, with average interprovincial flow directions from west to east
25 and south to north. About 56% of total green water exported from 31 mainland source
26 provinces remains at home, contributing to 43% of precipitation in China. The green
27 water from source provinces embodies substantial socio-economic values for
28 downwind provinces, accounting for about 40% of water resources, 45% of GDP, 46%

29 of population, and 50% of food production of China. Green water from western
30 provinces is the largest contributor to water resources, while green water from
31 southwestern and central provinces embodies the highest GDP, population, and food
32 production. Overall, the embodied socio-economic values of green water flow increase
33 from source to sink provinces, suggesting that green water from less developed
34 provinces effectively supports the higher socio-economic status of developed provinces.
35 The assessment emphasizes the substantial tele-connected socio-economic values of
36 green water flows and the need to incorporate them toward a more comprehensive and
37 effective water resources management.

38

39 **1 Introduction**

40 Terrestrial moisture recycling is a crucial process of the water cycle, whereby
41 water evaporates from land into the atmosphere, travels with prevailing winds, and
42 eventually falls back to the land as precipitation (van der Ent et al., 2010; Keys and
43 Wang-Erlandsson, 2018; Zemp et al., 2014). Terrestrial evapotranspiration (i.e., green
44 water) (Falkenmark and Rockström, 2006), which includes evaporation and
45 transpiration from land and vegetation, contributes to over half of the global
46 precipitation on land (van der Ent et al., 2010; Theeuwes et al., 2023; Tuinenburg et al.,
47 2020). Green water flows from upwind source regions to generate precipitation and
48 supply water resources for the social development of downwind sink regions through
49 moisture recycling (Schyns et al., 2019; Wang-Erlandsson et al., 2022). Analogous to
50 the upstream and downstream connection via blue water (referring to surface water and
51 groundwater flow within a watershed (Gleeson et al., 2020), the upwind source and
52 downwind sink regions are connected via green water flow within the evaporationshed
53 (i.e., downwind regions receiving precipitation from a specific location's evaporation)
54 (Ent and Savenije, 2013). Changes in both blue and green water flow directly impact
55 water resources availability, thereby influencing regional water security and human
56 societies (Keys et al., 2019).

57 The blue and green water flows provide a mechanism through which
58 upstream/upwind changes in ecohydrological and societal processes may affect the
59 downwind/downstream supply of water resources and, thus, ecological and societal
60 systems therein. Due to upstream water withdrawal and dams, global total blue water
61 flow into oceans and internal sinks decreased by 3.5% in 2002 compared to 1961–1990
62 (Döll et al., 2009). The decline in water availability exacerbated water stress in

63 downstream of transboundary river basins (Munia et al., 2016). Moreover, upstream
64 vegetation restoration, soil and water conservation practices reduced water yield
65 downstream, as already happened in the Yellow River (Wang et al., 2017; Zhou et al.,
66 2015b). Numerous studies have investigated the causal connection of blue water flow
67 from upstream and downstream regions, yet research into the connection of green water
68 flow from upwind and downwind regions and their impacts remains inadequate.

69 Unlike blue water flow primarily shaped by terrain with specific routes and
70 regulated by human activities (e.g., reservoir, transfer), green water flow is transported
71 by atmospheric air movement in a pervasive manner from evapotranspiration to
72 precipitation in downwind sink regions (Schyns et al., 2019). This establishes a spatial
73 linkage between source and sink regions for green water flow through the moisture
74 recycling process, similar to blue water flow through the surface hydrological process.
75 Therefore, evapotranspiration changes associated with land cover changes in source
76 regions are likely to impact not only downstream rivers via blue water flow but also
77 downwind precipitation via green water flow (Keys et al., 2012), with further
78 implications on socio-economic development (Wang-Erlandsson et al., 2018). For
79 example, vegetation greening reduced blue water but increased downwind water
80 availability globally through green water (Cui et al., 2022). Reduction in green water
81 in Amazon decreased downwind precipitation in the United States (Lawrence and
82 Vandecar, 2015), and reduction in green water source regions could decrease potential
83 crop yields in key global food-producing regions (Bagley et al., 2012).

84 Source regions supply water resources to support sink regions' socio-economic
85 development through both blue and green water flows. Existing research has
86 extensively assessed the socio-economic values of blue water, e.g., the population
87 dependency on runoff (Green et al., 2015; Viviroli et al., 2020), while seldom
88 considering the tele-connected effects of green water on socio-economy. In fact, green
89 water is also closely tied to human society because green water traveling from source
90 regions precipitates, recharges water resources, and ultimately sustains socio-economic
91 activities, livelihoods, and ecosystems in sink regions (Aragão, 2012; Keys and Wang-
92 Erlandsson, 2018; O'Connor et al., 2021). These contributions should be quantified and
93 recognized as the value of green water to socio-economy, which expands the scope of
94 water management and water security maintenance (Keys et al., 2017; Rockström et al.,
95 2023). Emerging moisture tracking technologies offer feasible ways to quantify green
96 water flow across regions at large scale (Keys et al., 2019; Li et al., 2023; Theeuwens et

97 al., 2023) and pave the way for assessing the socio-economic values of green water.

98 The general spatial and seasonal patterns of moisture flows in China are
99 determined by regional atmospheric circulation systems, including prevailing westerly
100 winds (from the west toward the east) in most of China between 30° and 60° (Bridges
101 et al., 2023), the East Asian monsoon in eastern China, and India monsoon in
102 southwestern China. In summer, the East Asian and Indian monsoons supply moisture
103 for precipitation in eastern and southwestern China (Tian and Fan, 2013). In winter, the
104 East Asian monsoon drives northwesterly moisture transport across much of China and
105 generates precipitation (Wu and Wang, 2002). Recent studies analyzed the large-spatial
106 pattern of moisture recycling in China at the grid (Zhang et al., 2023a), river basin
107 (Wang et al., 2023b), and ecological regions scales (Xie et al., 2024), or for specific
108 regions (Pranindita et al., 2022; Zhang et al., 2024). However, green water flows from
109 different regions are interlinked and become sources and sinks of each other. Such green
110 water transfer at a sub-national scale effectively forms an interconnected green water
111 flow network. It highlights the mutual dependency of green water and its socio-
112 economic contributions, especially for large countries like China. Few studies focus on
113 green water flows at the administrative district scale, which is important for water
114 management. Furthermore, the substantial regional disparities in socio-economic
115 development add complexity to understanding the socio-economic contributions of
116 green water among Chinese provinces. The western provinces with a weak economic
117 status and sparse populations are abundant in water resources (Ya-Feng et al., 2020). In
118 contrast, the economically developed and densely populated eastern provinces suffer
119 from water scarcity (Varis and Vakkilainen, 2001). Therefore, quantifying
120 interprovincial green water flows and evaluating the embedded socio-economic values
121 offer new perspectives for optimizing water resource utilization and mitigating the
122 imbalance in regional socio-economic development.

123 In this study, we used a high-quality moisture trajectory dataset from the UTrack
124 model to quantify and visualize the interprovincial network of green water flows within
125 China. Next, we combined socio-economic statistical data to evaluate socio-economic
126 values embodied in green water flow for economic production, population and food
127 production. Our study aims to reveal the transboundary green water flows within China
128 and their tele-connected effects on the socio-economy. This study incorporates green
129 water flow into water resources, extending water resources management beyond blue
130 water toward a more complete understanding of the water cycle and its socio-economic

131 implications, which is beneficial to assess and optimize regional water security.

132 **2 Data and Methods**

133 **2.1 Data**

134 This study used the moisture trajectory dataset generated by the Lagrangian
135 moisture tracking model “UTrack-atmospheric-moisture” driven by ERA5 reanalysis
136 data. The model is the state-of-the-art moisture tracking model, producing more
137 detailed evaporation footprints due to the high spatial resolution and reduced
138 unnecessary complexity (Tuinenburg and Staal, 2020). The dataset provides monthly
139 mean moisture flows at the global scale with a spatial resolution of 0.5° for 2008–2017,
140 expressed as the fractions of evaporation from a source grid allocated to precipitation
141 at a sink grid (Tuinenburg et al., 2020). It has been widely used in moisture recycling
142 research with various spatial scales, such as precipitation source of the grid (Staal et al.,
143 2023; Wei et al., 2024; Zhang et al., 2023a) and basin scale (Wang et al., 2023b), and
144 moisture transport between nations (Rockström et al., 2023). The moisture trajectory
145 dataset was used in conjunction with the multi-year monthly mean ET of 2008–2017
146 from the ERA5 reanalysis dataset to estimate precipitation in a sink grid originating
147 from a source grid.

148 The socio-economic statistical data in 2008–2017 from the China Statistical
149 Yearbook were used to estimate the socio-economic values of green water in terms of
150 water resources volume, gross domestic product (GDP), population, and food
151 production for 31 provinces in mainland China, without Hong Kong, Macau, and
152 Taiwan due to the data limitation. GDP was adjusted to price in the year 2020 to
153 eliminate the effects of inflation.

154 **2.2 Quantify green water flows in China**

155 We quantified interprovincial moisture flows and their precipitation contribution
156 following the workflow described in Fig. A1. At each sink grid, the
157 ~~ET~~evapotranspiration (ET) to precipitation (ET-to-P) fractions from the moisture
158 trajectory datasets were multiplied by ERA5 ~~evapotranspiration (ET)~~ET to obtain
159 monthly precipitation contribution by moisture from its source grids. Repeating the
160 calculation for all grids within a sink province and summing them up yielded the
161 precipitation in the sink province contributed by each source grid (Fig. A1 Step 1). Next,
162 we employed zonal statistics to sum up precipitation in the sink province contributed
163 by grids of each source province, and the precipitation contribution was converted to
164 relative values, i.e., the fraction of precipitation in sink province j originating from

165 green water of a source province i (denoted as W_{ij}) rather than absolute contribution to
 166 reduce the uncertainty in the latter (Fig. A1 Step 2). The fractions W_{ij} multiplied by the
 167 observed precipitation of the sink province restore the absolute precipitation
 168 contribution. This practice ensures that provincial precipitation is fully decomposed
 169 into different sources, ~~avoiding reducing~~ the estimation bias of sink precipitation due to
 170 unclosed water balance by ET and precipitation data (De Petrillo et al., 2024). Finally,
 171 the interprovincial green water flows in China were derived after estimating each
 172 province individually.

173 The direction of green water flows can be represented by a vector starting from a
 174 source to sink province determined by their geometric centers and with its length
 175 denoting flow magnitude. Since green water flows have multiple destinations, each
 176 flow points to different sink provinces, and even outside of China. For each source
 177 province, all of their domestic green water flow vectors can be averaged to a composite
 178 to represent their net direction and magnitude, which are mainly determined by
 179 atmospheric wind conditions, source location and green water volume.

180 **2.3 Quantify socio-economic values embodied in green water**

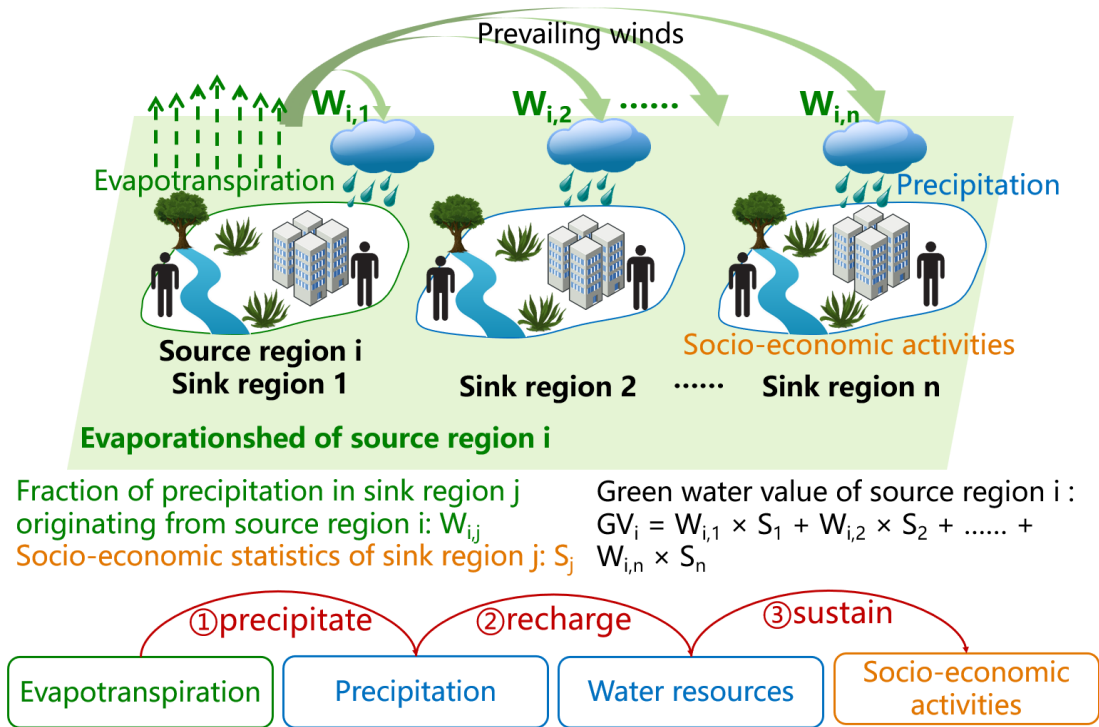


Figure 1. A conceptual diagram depicts the teleconnection of green water flows and their socio-economic contributions in a cascade manner. Evapotranspiration (green dotted arrows) from source region i flows downwind with prevailing winds (green thick arrows) and precipitates in sink region n , which recharges water sources and sustains socio-economic activities in sink regions.

187 Green water from upwind source provinces flows and precipitates downwind to
 188 recharge water resources, and therefore sustains socio-economic activities in sink
 189 provinces, as depicted in Fig. 1. Consequently, precipitation, water resources, and
 190 socio-economic factors such as economic activities, human livelihood, and crop
 191 production in sink provinces rely on green water exported from source provinces.
 192 Changes in green water may affect water resource volume, and then impact economic
 193 activities, livelihood, and crop production through water supply. We chose water
 194 resources volume, economic output (measured by GDP), population, and food
 195 production as the four socio-economic indicators that are tightly related to water
 196 resources to evaluate the socio-economic contributions of green water.

197 If we assume all socio-economic activities in sink province j are sustained by
 198 precipitation which constitutes water resources and recharges groundwater, socio-
 199 economic statistics of sink province j can be partitioned to source provinces by their
 200 share of precipitation contribution (W_{ij}). Therefore, multiplying socio-economic
 201 statistics in sink province j (S_j) by W_{ij} yielded the socio-economic value of green water
 202 from source province i . The total socio-economic value of green water of source
 203 province i (GV_i) can be obtained by summing its contributions to all sink provinces (Fig.
 204 1), as equation (1):

$$205 \quad GV_i = \sum_{j=1}^n (W_{i,j} \times S_j), \quad (1)$$

206 where S_j is the average socio-economic value of 2008-2017 (i.e., water resources
 207 volume (km^3), GDP (in unit of CNY, 1 CNY = 0.14 USD), population (persons), and
 208 food production (ton)) at sink province j , n is the number of sink provinces.

209 Due to the different socio-economic development statuses, the same amount of
 210 green water may produce different socio-economic values between source and sink
 211 provinces. This means green water flow also involves changes in embodied socio-
 212 economic value from source to sink provinces. We used water productivity in the source
 213 province (WP_i) to calculate the socio-economic values of its exported green water in
 214 the counterfactual scenario when it was all consumed in the source province without
 215 interprovincial transfer (GV'_i) (Eq. 2). The results were compared with the actual green
 216 water's socio-economic values (Eq. 1) (namely socio-economic values of exported
 217 green water when it is consumed in sink provinces) as:

$$218 \quad GV'_i = \sum_{j=1}^n (W_{i,j} \times WU_j \times WP_i), \quad (2)$$

219 where WU_j is water use in sink province j , and WP_i is water productivity in source
 220 province i . (i.e., economic output, population, and food production per unit water use).

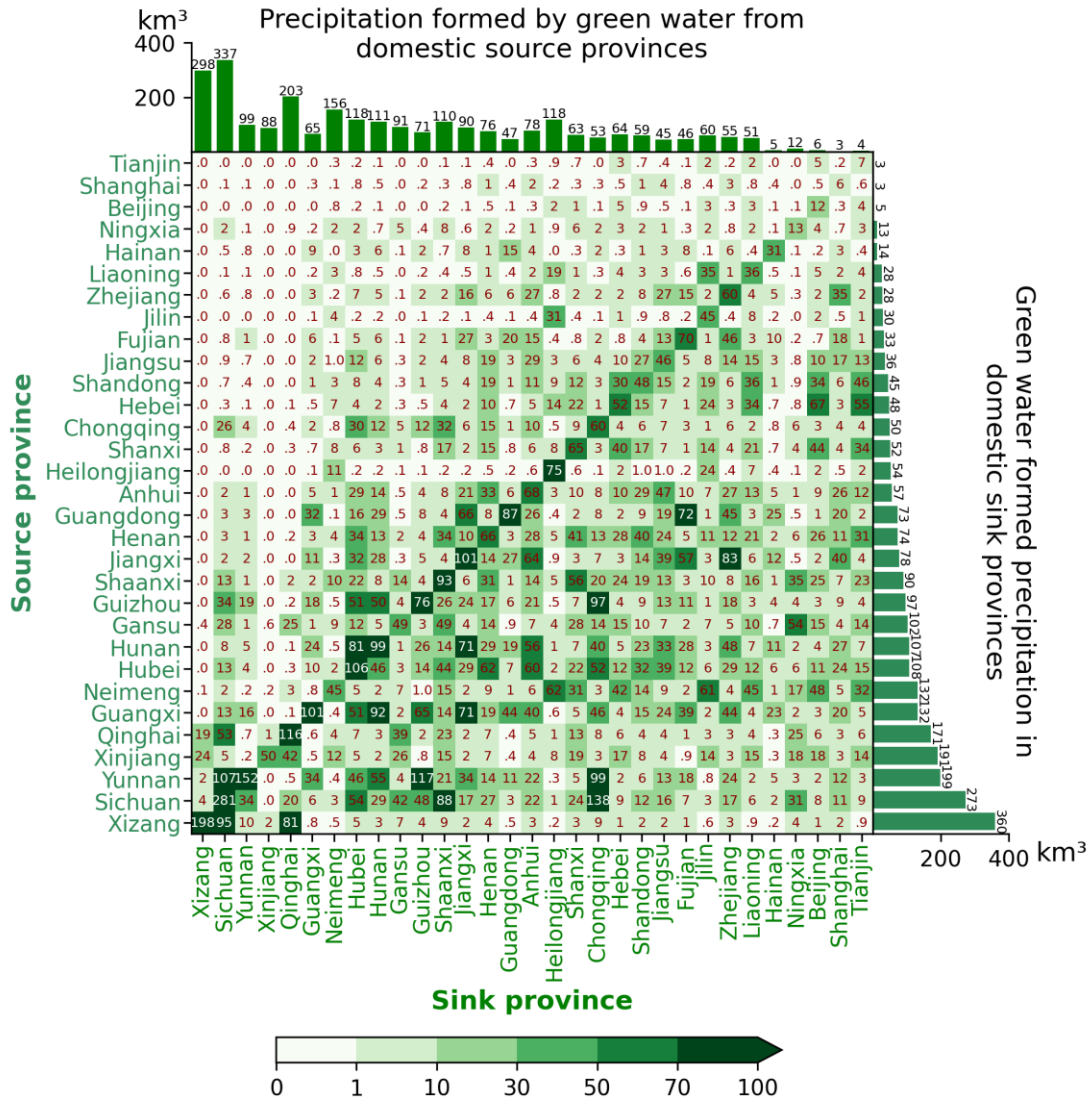
221 The changes in the socio-economic value of green water flow (ΔGV_i) from source
222 province i to its sink provinces can be estimated by Eq. 3.

223
$$\Delta GV_i = GV_i - GV'_i \quad (3)$$

224 $\sum_{i=1}^n \Delta GV_i$ is the net change in socio-economic values of all interprovincial
225 green water flows in China.

226 **3 Results**

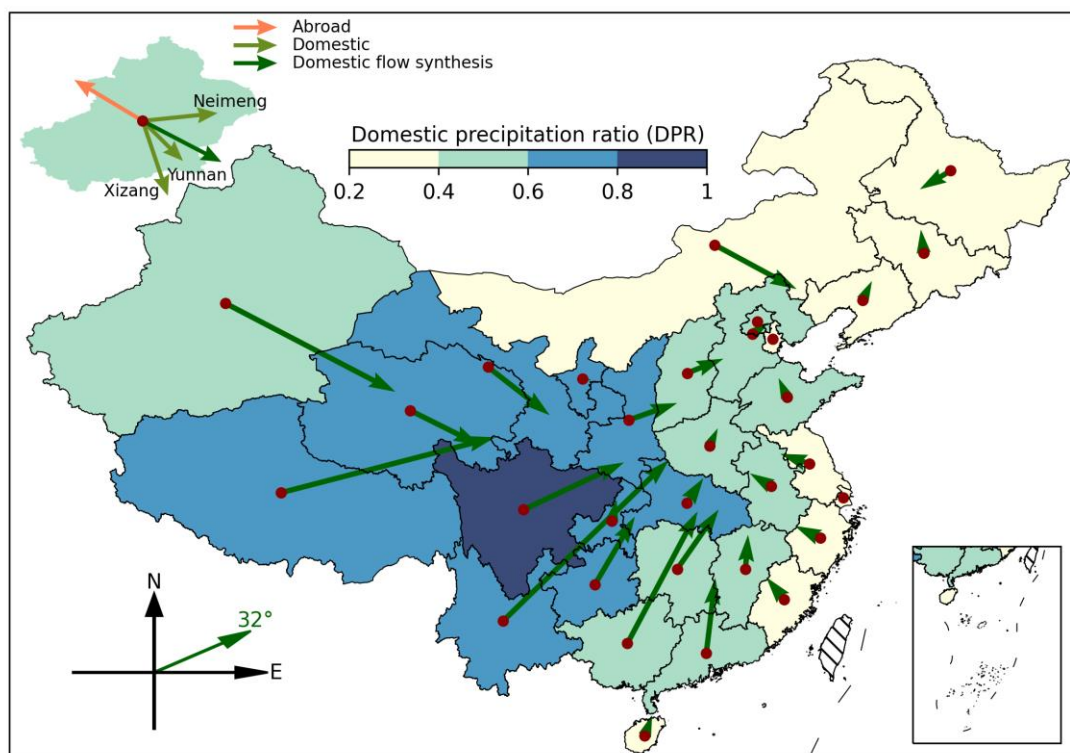
227 **3.1 The interprovincial green water flows in China and their directions**



228 Precipitation formed by green water from source to sink provinces (mm)
229 Figure 2. Interprovincial green water flows in China. The heat map denotes precipitation in sink
230 province generated by green water from a source province (mm). The right bar shows domestic
231 precipitation (km^3) formed by green water from each source province. The top bar shows
232 precipitation in each sink province formed by green water from domestic source provinces (km^3).
233 Green water exported from a source province forms precipitation in different sink

234 provinces in China, and precipitation in a sink province originates from green water in
 235 different source provinces. Therefore, different provinces in China, acting either as
 236 sources or sinks, are interconnected through moisture recycling and established an
 237 interprovincial network (Fig. 2).

238 A large fraction of green water exported from each source province is retained
 239 locally to generate precipitation (diagonal cells in Fig. 2). The precipitation recycling
 240 ratio (PRR), the ratio of precipitation generated by local green water to total
 241 precipitation, reflects how much green water of each source province contributes to its
 242 own precipitation (Fig. A2c). Xizang has the highest PRR of 0.345, followed by
 243 Qinghai (0.341) and Sichuan (0.297). Besides local recycling, green water
 244 predominantly flows and generates more precipitation in neighboring provinces and
 245 less in distant provinces. For example, green water from Sichuan forms high
 246 precipitation in neighboring provinces such as Chongqing (138 mm), far surpassing
 247 other distant sink provinces (< 88 mm).



248
 249 Figure 3. Direction of green water flows from each source province in China. Green arrows
 250 indicate the average direction of domestic green water flows, denoted as a vector starting from a
 251 source (the geometric center in red points) to sink provinces and with its length representing the
 252 amount of precipitation formed by green water. The face colors on the map represent fractions of
 253 green water formed precipitation within China of each source province (DPR). The upper left
 254 corner is a schematic diagram for green water flows from Xinjiang. The lower left corner is the
 255 composite flow direction of interprovincial green water of all provinces.

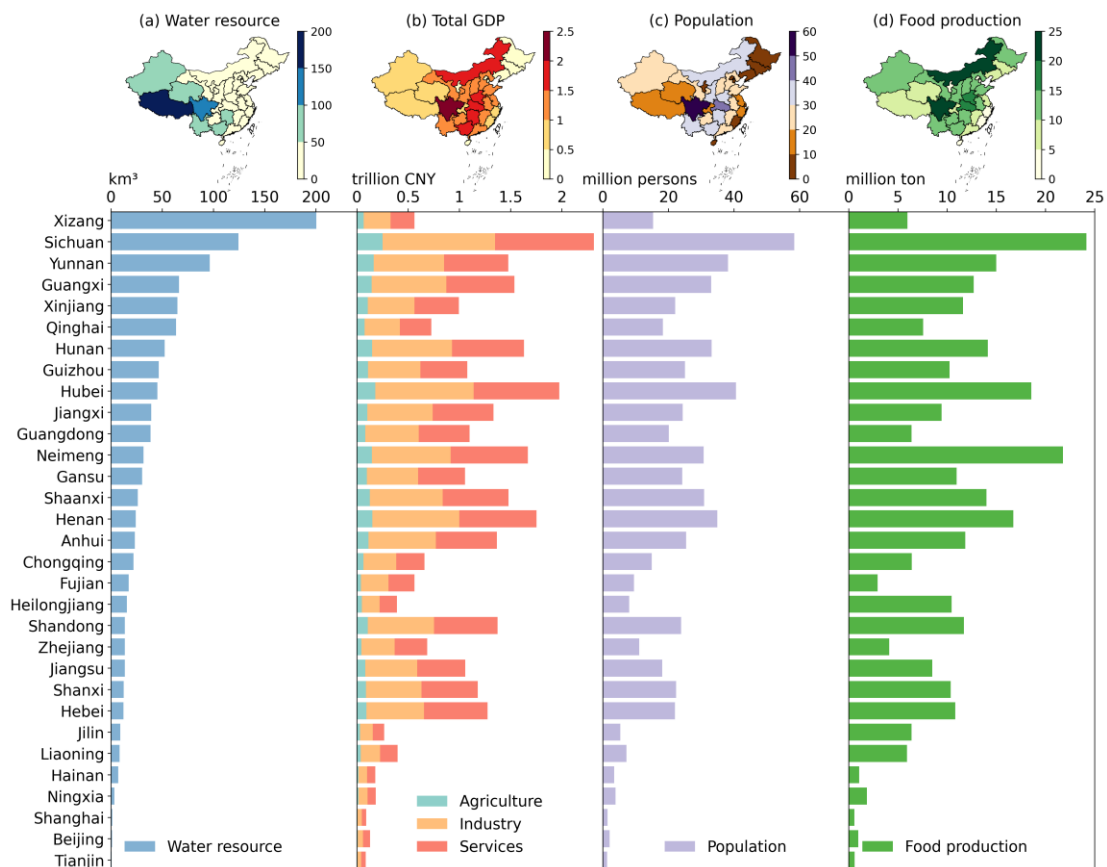
256 The direction of interprovincial green water flow can be visualized as a composite
257 direction averaging all domestic green water flows from each source province, which
258 are mainly determined by atmospheric wind conditions, source location, and green
259 water volume (Fig. 3). Overall, the average direction of all interprovincial green water
260 flows is at 32° northeastward (32° north off the east direction), suggesting green water
261 within China is transported to the north and east directions owing to combined effects
262 of monsoons and westerly.

263 Green water exported by source provinces contributes to precipitation both within
264 and outside China. We defined the domestic precipitation ratio (DPR) as the ratio of
265 green water that formed precipitation in China to each province's total green water
266 export to represent their relative importance to China's precipitation (Fig. A2a). Green
267 water from provinces in western and central China mainly flows eastward under the
268 influence of prevailing westerlies, which extend their evaporationsheds eastward to
269 cover a large territory of China and generate more precipitation within China (Fig. 3).
270 For instance, green water from Xizang, the largest exporter in China, produces the
271 largest domestic precipitation (360 km³) (right bar on Fig 2) with a high DPR of 0.74,
272 contributing to precipitation in other 30 provinces with varying extents (0.2 to 95 mm).
273 Similarly, the green water from southern provinces is affected by the Indian Ocean
274 Monsoon (southwest monsoon), which drives green water flowing northeastward. With
275 a substantial volume of green water, these southern provinces contribute significantly
276 to domestic precipitation. In contrast, green water from eastern coastal or northwest
277 border provinces goes to the northwest primarily attributed to the East Asian Monsoon
278 (southeast monsoon) (Cai et al., 2010). As a result, most evaporationsheds laid outside
279 China generate less domestic precipitation but more outside the country, resulting in a
280 lower DPR, such as Fujian (DPR 0.31) and Heilongjiang (DPR 0.23). The northern
281 provinces are influenced by westerly winds and winter monsoon from Siberia (Sun et
282 al., 2012), causing predominantly southeastward flow of green water. However,
283 evaporationsheds of these provinces mainly cover the Pacific Ocean, resulting in a
284 relatively low DPR despite their substantial volume of exported green water. While
285 some inland provinces have a high DPR because their evaporationsheds overlap with
286 mainland China, the low green water volume (Fig. A4) limits their domestic
287 precipitation contribution (e.g., Gansu and Ningxia with DPR of 0.72 and 0.66,
288 respectively).

289 Furthermore, precipitation in sink provinces originates from both domestic and

290 foreign green water sources. Sichuan (337 km³), Xizang (298 km³), and Qinghai (203
 291 km³) are the top 3 provinces importing the largest volume of green water from domestic
 292 sources due to the large ET from themselves and neighboring provinces (top bar of Fig
 293 2). To quantify the relative importance of domestic sources, we defined the domestic
 294 source ratio (DSR) in each province as the sum of precipitation contribution from
 295 domestic sources divided by total precipitation (Fig. A2 (b)). DSR is related to each
 296 province's precipitationshed (i.e., upwind region contributing evaporation to a specific
 297 location's precipitation) (Keys et al., 2014) and the included domestic green water
 298 exporters. The highest DSR found in Qinghai (0.86) and Ningxia (0.82) is because their
 299 precipitationsheds include large domestic green water exporters like Xinjiang and
 300 Xizang, which supply considerable green water traveling eastward. Conversely, Hainan
 301 (0.07) and Guangdong (0.14) in coastal areas have lower DSR because their
 302 precipitationsheds are primarily located in oceans and other countries due to the
 303 influence of the summer monsoon (Cai et al., 2010).

304 3.2 Socio-economic values embodied in interprovincial green water 305 flows



306
 307 Figure 4. The embodied socio-economic values of green water flow from source provinces for
 308 water resources, GDP, population, and food production (average value of 2008-2017) of sink
 309 provinces in China.

310 Source provinces export green water and create precipitation to sink provinces
311 through moisture recycling process, recharging water resources and sustaining the
312 socio-economic development of downwind sink provinces (Fig. 4). The reliance of
313 socio-economic activities in sink provinces on green water supply from source
314 provinces implies that the green water and socio-economy are intertwined through the
315 interprovincial green water flow network, indicating a teleconnection between source
316 and sink provinces.

317 Our assessment of contribution of green water to water resources indicates that
318 green water from western provinces recharges the highest volume of water resources.
319 Xizang (200 km³), Sichuan (124 km³), and Yunnan (96 km³) are the top 3 contributors
320 of water resources, whose green water export makes up 46%, 51%, and 52% of their
321 own total water resources, respectively (Table. A1). These regions also correspond to
322 the top contributors to domestic precipitation, owing to the close linkage between
323 precipitation and water resources. Although southern and eastern provinces are rich in
324 water resources due to the wet climate, most of their green water contributes to water
325 resources outside of China or to the ocean since they are situated downwind of
326 prevailing westerlies and proximate to the coast (e.g., Guangdong). In total, green water
327 exported from 31 provinces contributes 43% and 40% of precipitation and water
328 resources in China (Table. A1).

329 The GDP, population, and food production embodied in green water export from
330 source provinces are shown in Fig 5b-d, which reflects how much the socio-economy
331 of downwind sink provinces is supported by green water of source provinces. Overall,
332 the contribution of green water to selected socio-economic statistics shows similar
333 rankings because food production and agriculture GDP ($R = 0.79$), population and total
334 GDP ($R = 0.85$) are spatially correlated (Fig. A6).

335 Sectoral GDP embodied in green water from source provinces is highly related to
336 the industrial structure in sink provinces. The embodied industry and service sector
337 GDP values across provinces are relatively comparable, whereas embodied agricultural
338 GDP values are lower due to the small percentage of agricultural output to total GDP
339 (Fig. A3).

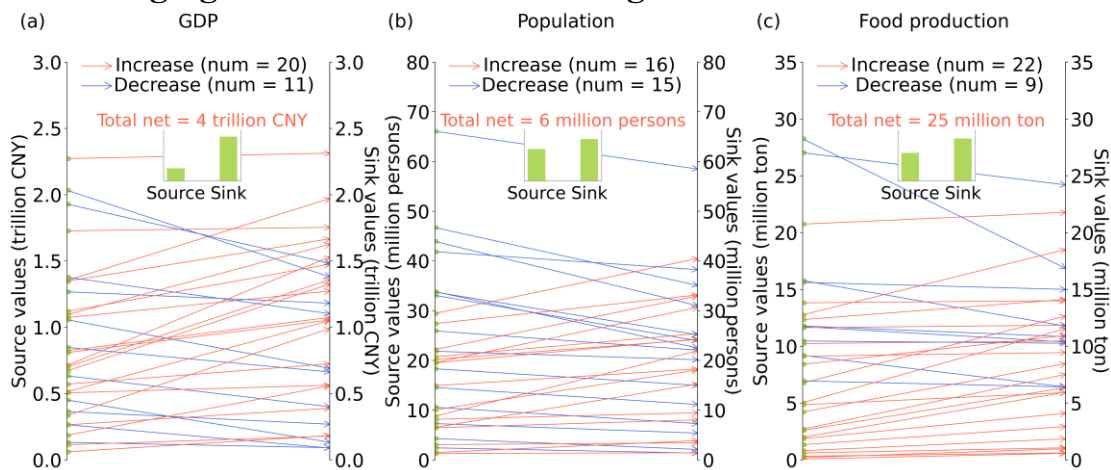
340 Green water from southwest and central provinces (e.g., Sichuan, Hubei, Henan)
341 embodies the most GDP, population, and food production because of the large
342 economic volume of these provinces and neighboring regions, as well as the high DPR.
343 Specifically, green water from Sichuan supports the highest GDP (2.31 trillion CNY),

344 population (58 million persons), and food production (24 million tons) (Table. A2)
 345 because Sichuan has a high GDP, population, and food production (Fig. A3). Moreover,
 346 green water from Sichuan contributes significantly to its own precipitation (30%), and
 347 87% of its green water generates domestic precipitation. These factors together make
 348 green water in provinces like Sichuan embody the highest socio-economic values.

349 Provinces that export large volumes of green water and have high DPR do not
 350 necessarily embody more socio-economic values if sink provinces that import their
 351 green water are less developed. Xizang is the highest green water exporter and the
 352 largest contributor of water resources (200 km³) but ranks low in embodied GDP (0.56
 353 trillion CNY, 23rd), population (15 million, 20th), and food production (5.97 million tons,
 354 23rd) because the primary importer of its green water, such as Xizang and Qinghai, have
 355 low rankings in GDP (31st, 30th), population (31st and 30th), and food production (30th
 356 and 29th).

357 Green water from highly developed provinces (e.g., southeastern China) may not
 358 necessarily embody high socio-economic value if they have low DPR. For example,
 359 Guangdong ranks 1st in GDP and population and 17th in food production but only has a
 360 small fraction of green water contributing to domestic precipitation (DPR 0.4). The
 361 limited domestic precipitation contribution results in low rankings of embodied socio-
 362 economic values (14th for GDP, 17th for population, and 21st for food production) for
 363 Guangdong.

364 3.3 Changing socio-economic values of green water flows



365
 366 Figure 5. Changes in socio-economic values embodied in green water flow from source to sink
 367 provinces for GDP (a), population (b), and food production (c). Thin arrows of different colors
 368 represent the socio-economic value increase (in red) or decrease (in blue) from source to sink
 369 provinces. Green bars represent the sum socio-economic value in China's 31 provinces.

370 The substantial socio-economic values embodied in interprovincial green water

371 flows highlight the teleconnection of green water from source provinces and the socio-
372 economy in sink provinces, including economy, population, and food production. Due
373 to different socio-economic statuses, the same amount of consumed water resources,
374 which are recharged by green water, would sustain different socio-economic values
375 between source and sink provinces. Therefore, the socio-economic values embodied in
376 green water flow would change when traveling from source to sink provinces. As shown
377 in Fig. 5, the socio-economic values embodied in green water flow increase from source
378 to sink provinces by 4 trillion CNY for GDP, 6 million for population, and 25 million
379 tons for food production, respectively. The increase in the embodied GDP, population,
380 and food production is observed in 20, 16, and 22 source provinces among a total of 31.
381 This indicates that green water tends to flow from less to more developed provinces,
382 sustaining more economic production, population, and food production per unit of
383 green water. The largest economic output value increases are in Guangxi (+0.83 trillion
384 CNY, 54%). Xinjiang has the most added value in population (+13 million persons,
385 59%) and food production (+7 million tons, 60%) because their green water flows to
386 more developed provinces (Fig. A5). In contrast, decreased socio-economic values of
387 green water flow are also observed. Shandong, Shaanxi, and Henan have the largest
388 depreciation in green water values for GDP (-0.66 trillion CNY, 48%), population (-13
389 million persons, 42%), and food production (-12 million tons, 72%) (Fig. A5) because
390 their green water flows to provinces with lower socio-economic values.

391 The changing socio-economic values of green water flow reflect the regional
392 disparity in socio-economic statuses between source and sink provinces. The exported
393 green water for more than half of the source provinces in China (> 15) has increased
394 socio-economic values when reaching sink provinces. This shows that green water from
395 less developed provinces effectively supports the higher socio-economic status of
396 developed provinces through the interprovincial flow network. Therefore, these
397 provinces are vitally important green water providers to developed areas. This
398 teleconnection of green water and socio-economy substantiates that changing land use
399 in the source provinces that affect evapotranspiration is likely to influence water
400 resources availability and socio-economic development in the sink provinces (Dias et
401 al., 2015; Weng et al., 2018). Hence, it is imperative to account for “invisible” green
402 water flow and its cascade effect in large-scale water resources management.

403 **4 Discussion**

404 This study quantified the interprovincial green water flows in China using the

405 moisture recycling framework and a moisture tracking model. The green water flow is
406 established by transporting evaporated moisture by atmospheric winds from a source
407 province to precipitate in a sink province. The transferred green water exchanges among
408 multiple provinces and creates an interprovincial flow network. The location of the
409 source province and its flow direction largely determine to what extent green water
410 formed precipitation retains within China. In our estimation, roughly 43% of green
411 water forms precipitation in China, similar to 44% of PRR identified by Rockström et
412 al. (2023). The average direction of all interprovincial green water flows in China is
413 from southwest to northeast, consistent with findings by Xie et al. (2024).

414 Green water flow can fill the gap in land-atmosphere feedback in the traditional
415 water resources management framework (Keys et al., 2017). Typically, water resources
416 management only considers blue water changes while neglecting green water flow,
417 even though the latter may compensate for the former (Hoek van Dijke et al., 2022).
418 Human activities such as irrigation (Su et al., 2021), afforestation (Li et al., 2018), and
419 reservoir construction (Biemans et al., 2011; Veldkamp et al., 2017) in upstream regions
420 may markedly change blue water accessibility in downstream regions. Meanwhile, the
421 resulting changes of ET in upstream regions (McDermid et al., 2023; Qin, 2021; Shao
422 et al., 2019) might offset the decline of water resources in downstream by moisture
423 recycling. Similarly, increased vegetation coverage intercepts more rainfall, reducing
424 runoff and consequently diminishing water resources availability (Sun et al., 2006;
425 Zhou et al., 2015a), but the rise of ET may compensate for local and downwind water
426 availability through increased green water flows (Wang et al., 2023a; Zhang et al.,
427 2021). Therefore, green water is an essential path of climatic and hydrological
428 interaction among different regions, providing a new angle for integrated regional
429 resources management (Keys et al., 2018; te Wierik et al., 2021). A comprehensive
430 impact assessment of regional water security and optimization would benefit from
431 combining both blue and green water flows (Schyns et al., 2019) by which
432 upstream/upwind regions affect regional water resource availability (Creed et al., 2019).

433 With the recognition of the tele-connected effects of green water flows,
434 maintaining regional water security requires both rational utilization of local water
435 resources and appropriate land management in the upwind source regions. However,
436 similar to blue water, water resource management across administrative boundaries has
437 always been challenging due to conflicting interests among different regions
438 (Rockström et al., 2023). The diverse strategies developed to enhance regional

439 coordination of blue water management serve as a reference for green water
440 management, such as the inter-basin water transfer or downstream beneficiaries paying
441 upstream providers for clean water services (Farley and Costanza, 2010; Pissarra et al.,
442 2021; Sheng and Webber, 2021). However, unlike blue water resources with well-
443 established accounting and valuation methods, green water monitoring and valuation
444 are challenging. Green water from a specific region flows to multiple regions, and the
445 received green water can subsequently reevaporate and flow to other regions (Zemp et
446 al., 2014). This interconnected network and cascade complicate the quantification of
447 how much green water from a source region contributes to human activities in sink
448 regions. More importantly, it is difficult to measure green water flow through
449 observations as those measurements made by hydrologic stations for blue water (Hu et
450 al., 2023; Sheng and Webber, 2021). This study utilized a dataset from a moisture
451 tracking model to construct an interprovincial green water flow within China, which
452 offers valuable insights for understanding the quantity of green water flow.

453 Due to the complex dynamics of the green water flow and limitations of the
454 moisture tracking model, there are still major uncertainties in data and methods of this
455 study. First, ET and precipitation datasets driving the UTrack model affect the tracked
456 trajectories and magnitude of moisture flow. The resulting moisture trajectory is
457 expressed as the ET-to-P fraction ~~of ET to precipitation~~, and the exact amount of
458 moisture is restored by the ET and precipitation datasets chosen by users. Different ET
459 and precipitation datasets could lead to different precipitation contributions and PRR
460 (Li et al., 2023). We used the ERA5 dataset to keep consistent with the original UTrack
461 model. It is noted that the non-closure of the moisturehydrological balance from ERA5
462 (De Petri et al., 2024) and divergence in moisture tracking models (e.g.,
463 simplifications and assumptions ~~introduced in the moisture tracking model~~) also add
464 uncertainty in ~~and impact the accuracy of the~~ moisture tracking ~~tracked green water flow~~
465 (Tuinenburg and Staal, 2020; Zhang et al., 2023b). Moreover, the resulting moisture
466 trajectory data only represent the climatologically average moisture trajectories and ET
467 (Li et al., 2023), neglecting the interannual variability in moisture flow trajectory, e.g.,
468 those induced by the influence of extreme weather events or ENSO (Zhao and Zhou,
469 2021). The interannual variations in green water flow may affect DPR and DSR in some
470 provinces. Human adaptation tends to buffer the impacts of interannual variations on
471 the socio-economy through water resource management such as reservoirs, dams, and
472 other infrastructure. Accounting for interannual variations in green water flows and

473 their socio-economic contribution is worth further investigation. Secondly, the socio-
474 economic value assessment of green water in this study only considers green water
475 flows within China, excluding flows moving abroad and to the ocean that may embody
476 socio-economic value beyond the territory of mainland China. We mainly attribute
477 socio-economic values to green water and generated precipitation because precipitation
478 is the ultimate water source for recharging surface and groundwater of a region. Strictly
479 speaking, such attribution needs to be more precise because socio-economy also utilizes
480 streamflow from upstream areas, which deserve separate attention.

481 Moreover, the interactions between blue and green water increase the complexity
482 to evaluating green water's socio-economic contribution. For example, the blue water
483 extracted by irrigation increases ET in the source region, providing more moisture for
484 downwind regions (Yang et al., 2019). Simultaneously, most of the blue water for local
485 irrigation comes from the green water of upwind regions (McDermid et al., 2023). In
486 addition, not all water resources replenished by green water-induced precipitation are
487 accessible for human activities since part of them is used by the natural ecosystem
488 (Keys et al., 2019). Therefore, it is necessary to distinguish water sources and
489 consumption to account green water values more accurately. Despite the selected socio-
490 economic indicators closely linked to water resources, green water flows' socio-
491 economic contribution can manifest in other aspects such as livestock production and
492 irrigated agriculture. In future studies, the dynamic linkage between green water, water
493 resources and economic development can be assessed annually by using a long-term
494 moisture tracking dataset with a separation of water sources consumed by socio-
495 economy (surface and groundwater). Nevertheless, our assessment serves as a useful
496 first step to demonstrate the importance of the tele-connected green water flow in
497 addition to blue water. Our attempts to quantify the socio-economy embodied in green
498 water flow fill the gap in green water value assessment and provide a methodological
499 reference for green water management.

500 **5 Conclusion**

501 This study quantified the interprovincial green water flows in China and its tele-
502 connected effects on the socio-economy. The green water exchanges among different
503 regions effectively form a complex flow network and embody socio-economic values.
504 The interprovincial green water in China flows primarily from west to east and to a
505 lesser extent from south to north, influenced by the co-control of westerlies and
506 monsoons. Western provinces have significant contributions to precipitation and water

507 resources in China, while southwestern and central provinces have the most socio-
508 economic values regarding GDP, population, and food production. Green water flowing
509 from less developed regions supports substantial socio-economic values in more
510 affluent regions due to disparity in socio-economic development between source and
511 sink regions. Given the embodied socio-economic benefits of green water, regional
512 water resources management should consider water flow beyond blue water to integrate
513 green water for a more comprehensive and effective management of resources and
514 security. Our study provides a reference for understanding the “invisible” green water
515 flow and its tele-connected benefits.

516 **Data and code availability**

517 The moisture trajectory dataset is available at
518 <https://doi.pangaea.de/10.1594/PANGAEA.912710> (Tuinenburg et al.,
519 2020)(~~Tuinenburg et al., 2020~~). The evapotranspiration data from ERA5 reanalysis
520 dataset is available at [https://cds.climate.copernicus.eu/datasets/reanalysis-era5-single-](https://cds.climate.copernicus.eu/datasets/reanalysis-era5-single-levels-monthly-means?tab=overview)
521 [levels-monthly-means?tab=overview](https://cds.climate.copernicus.eu/datasets/reanalysis-era5-single-levels-monthly-means?tab=overview) (Hersbach et al., 2023). The socio-economic
522 statistics data is available from China Statistical Yearbook
523 (<https://data.stats.gov.cn/index.htm>).

524 The Python codes and data used in this study are available at GitHub
525 (<https://github.com/sangshan-ss/GW-China>).

526 **Author contributions**

527 YL and SS conceived the study and performed data analysis. SS and YL wrote the
528 manuscript with contributions from CCH, SSZ and HQL.

529 **Competing interests**

530 We declare no conflict of interest of this work.

531 **Financial support**

532 This research was funded by the National Natural Science Foundation of China
533 (42041007), the Second Tibetan Plateau Scientific Expedition and Research Program
534 (2019QZKK0405) and the Fundamental Research Funds for the Central Universities.

535 **References**

536 Aragão, L. E. O. C.: The rainforest’s water pump, *Nature*, 489, 217–218,
537 <https://doi.org/10.1038/nature11485>, 2012.

538 Bagley, J. E., Desai, A. R., Dirmeyer, P. A., and Foley, J. A.: Effects of land cover
539 change on moisture availability and potential crop yield in the world’s breadbaskets,
540 *Environ. Res. Lett.*, 7, 014009, <https://doi.org/10.1088/1748-9326/7/1/014009>, 2012.

541 Biemans, H., Haddeland, I., Kabat, P., Ludwig, F., Hutjes, R. W. A., Heinke, J.,
542 Bloh, W. von, and Gerten, D.: Impact of reservoirs on river discharge and irrigation

- 543 water supply during the 20th century, *Water Resources Research*, 47,
544 <https://doi.org/10.1029/2009WR008929>, 2011.
- 545 Bridges, J. D., Tarduno, J. A., Cottrell, R. D., and Herbert, T. D.: Rapid
546 strengthening of westerlies accompanied intensification of Northern Hemisphere
547 glaciation, *Nat Commun*, 14, 3905, <https://doi.org/10.1038/s41467-023-39557-4>, 2023.
- 548 Cai, Y., Tan, L., Cheng, H., An, Z., Edwards, R. L., Kelly, M. J., Kong, X., and
549 Wang, X.: The variation of summer monsoon precipitation in central China since the
550 last deglaciation, *Earth and Planetary Science Letters*, 291, 21–31,
551 <https://doi.org/10.1016/j.epsl.2009.12.039>, 2010.
- 552 Creed, I. F., Jones, J. A., Archer, E., Claassen, M., Ellison, D., McNulty, S. G., van
553 Noordwijk, M., Vira, B., Wei, X., Bishop, K., Blanco, J. A., Gush, M., Gyawali, D.,
554 Jobbágy, E., Lara, A., Little, C., Martin-Ortega, J., Mukherji, A., Murdiyarsa, D., Pol,
555 P. O., Sullivan, C. A., and Xu, J.: Managing Forests for Both Downstream and
556 Downwind Water, *Front. For. Glob. Change*, 2,
557 <https://doi.org/10.3389/ffgc.2019.00064>, 2019.
- 558 Cui, J., Lian, X., Huntingford, C., Gimeno, L., Wang, T., Ding, J., He, M., Xu, H.,
559 Chen, A., Gentine, P., and Piao, S.: Global water availability boosted by vegetation-
560 driven changes in atmospheric moisture transport, *Nat. Geosci.*, 15, 982–988,
561 <https://doi.org/10.1038/s41561-022-01061-7>, 2022.
- 562 De Petrillo, E., Fahrländer, S., Tuninetti, M., Andersen, L. S., Monaco, L., Ridolfi,
563 L., and Laio, F.: Reconciling tracked atmospheric water flows to close the global
564 freshwater cycle, <https://doi.org/10.21203/rs.3.rs-4177311/v2>, 30 April 2024.
- 565 Dias, L. C. P., Macedo, M. N., Costa, M. H., Coe, M. T., and Neill, C.: Effects of
566 land cover change on evapotranspiration and streamflow of small catchments in the
567 Upper Xingu River Basin, Central Brazil, *Journal of Hydrology: Regional Studies*, 4,
568 108–122, <https://doi.org/10.1016/j.ejrh.2015.05.010>, 2015.
- 569 Döll, P., Fiedler, K., and Zhang, J.: Global-scale analysis of river flow alterations
570 due to water withdrawals and reservoirs, *Hydrology and Earth System Sciences*, 13,
571 2413–2432, <https://doi.org/10.5194/hess-13-2413-2009>, 2009.
- 572 Ent, R. J. van der and Savenije, H. H. G.: Oceanic sources of continental
573 precipitation and the correlation with sea surface temperature, *Water Resources*
574 *Research*, 49, 3993–4004, <https://doi.org/10.1002/wrcr.20296>, 2013.
- 575 van der Ent, R. J., Savenije, H. H. G., Schaeffli, B., and Steele-Dunne, S. C.: Origin
576 and fate of atmospheric moisture over continents, *Water Resources Research*, 46,
577 <https://doi.org/10.1029/2010WR009127>, 2010.
- 578 Falkenmark, M. and Rockström, J.: The New Blue and Green Water Paradigm:
579 Breaking New Ground for Water Resources Planning and Management, *Journal of*
580 *Water Resources Planning and Management*, 132, 129–132,
581 [https://doi.org/10.1061/\(ASCE\)0733-9496\(2006\)132:3\(129\)](https://doi.org/10.1061/(ASCE)0733-9496(2006)132:3(129)), 2006.
- 582 Farley, J. and Costanza, R.: Payments for ecosystem services: From local to global,
583 *Ecological Economics*, 69, 2060–2068, <https://doi.org/10.1016/j.ecolecon.2010.06.010>,
584 2010.
- 585 Gleeson, T., Wang-Erlandsson, L., Zipper, S. C., Porkka, M., Jaramillo, F., Gerten,
586 D., Fetzer, I., Cornell, S. E., Piemontese, L., Gordon, L. J., Rockström, J., Oki, T.,
587 Sivapalan, M., Wada, Y., Brauman, K. A., Flörke, M., Bierkens, M. F. P., Lehner, B.,
588 Keys, P., Kummu, M., Wagener, T., Dadson, S., Troy, T. J., Steffen, W., Falkenmark,

- 589 M., and Famiglietti, J. S.: The Water Planetary Boundary: Interrogation and Revision,
590 *One Earth*, 2, 223–234, <https://doi.org/10.1016/j.oneear.2020.02.009>, 2020.
- 591 Green, P. A., Vörösmarty, C. J., Harrison, I., Farrell, T., Sáenz, L., and Fekete, B.
592 M.: Freshwater ecosystem services supporting humans: Pivoting from water crisis to
593 water solutions, *Global Environmental Change*, 34, 108–118,
594 <https://doi.org/10.1016/j.gloenvcha.2015.06.007>, 2015.
- 595 Hersbach, H., Bell, B., Berrisford, P., Biavati, G., Horányi, A., Muñoz Sabater, J.,
596 Nicolas, J., Peubey, C., Radu, R., Rozum, I., Schepers, D., Simmons, A., Soci, C., Dee,
597 D., and Thépaut, J.-N.: ERA5 monthly averaged data on single levels from 1940 to
598 present, Copernicus Climate Change Service (C3S) Climate Data Store (CDS),
599 <https://doi.org/10.24381/CDS.F17050D7>, 2023. (Accessed on 28-10-2024)
- 600 Hoek van Dijke, A. J., Herold, M., Mallick, K., Benedict, I., Machwitz, M., Schlerf,
601 M., Pranindita, A., Theeuwes, J. J. E., Bastin, J.-F., and Teuling, A. J.: Shifts in regional
602 water availability due to global tree restoration, *Nat. Geosci.*, 15, 363–368,
603 <https://doi.org/10.1038/s41561-022-00935-0>, 2022.
- 604 Hu, H., Tian, G., Wu, Z., and Xia, Q.: Cross-regional ecological compensation
605 under the composite index of water quality and quantity: A case study of the Yellow
606 River Basin, *Environmental Research*, 238, 117152,
607 <https://doi.org/10.1016/j.envres.2023.117152>, 2023.
- 608 Keys, P. W. and Wang-Erlandsson, L.: On the social dynamics of moisture
609 recycling, *Earth System Dynamics*, 9, 829–847, [https://doi.org/10.5194/esd-9-829-](https://doi.org/10.5194/esd-9-829-2018)
610 2018, 2018.
- 611 Keys, P. W., van der Ent, R. J., Gordon, L. J., Hoff, H., Nikoli, R., and Savenije,
612 H. H. G.: Analyzing precipitationsheds to understand the vulnerability of rainfall
613 dependent regions, *Biogeosciences*, 9, 733–746, [https://doi.org/10.5194/bg-9-733-](https://doi.org/10.5194/bg-9-733-2012)
614 2012, 2012.
- 615 Keys, P. W., Barnes, E. A., van der Ent, R. J., and Gordon, L. J.: Variability of
616 moisture recycling using a precipitationshed framework, *Hydrology and Earth System
617 Sciences*, 18, 3937–3950, <https://doi.org/10.5194/hess-18-3937-2014>, 2014.
- 618 Keys, P. W., Wang-Erlandsson, L., Gordon, L. J., Galaz, V., and Ebbesson, J.:
619 Approaching moisture recycling governance, *Global Environmental Change*, 45, 15–
620 23, <https://doi.org/10.1016/j.gloenvcha.2017.04.007>, 2017.
- 621 Keys, P. W., Wang-Erlandsson, L., and Gordon, L. J.: Megacity precipitationsheds
622 reveal tele-connected water security challenges, *PLOS ONE*, 13, e0194311,
623 <https://doi.org/10.1371/journal.pone.0194311>, 2018.
- 624 Keys, P. W., Porkka, M., Wang-Erlandsson, L., Fetzer, I., Gleeson, T., and Gordon,
625 L. J.: Invisible water security: Moisture recycling and water resilience, *Water Security*,
626 8, 100046, <https://doi.org/10.1016/j.wasec.2019.100046>, 2019.
- 627 Lawrence, D. and Vandecar, K.: Effects of tropical deforestation on climate and
628 agriculture, *Nature Clim Change*, 5, 27–36, <https://doi.org/10.1038/nclimate2430>, 2015.
- 629 Li, Y., Piao, S., Li, L. Z. X., Chen, A., Wang, X., Ciais, P., Huang, L., Lian, X.,
630 Peng, S., Zeng, Z., Wang, K., and Zhou, L.: Divergent hydrological response to large-
631 scale afforestation and vegetation greening in China, *Science Advances*, 4, eaar4182,
632 <https://doi.org/10.1126/sciadv.aar4182>, 2018.
- 633 Li, Y., Xu, R., Yang, K., Liu, Y., Wang, S., Zhou, S., Yang, Z., Feng, X., He, C.,

- 634 Xu, Z., and Zhao, W.: Contribution of Tibetan Plateau ecosystems to local and remote
635 precipitation through moisture recycling, *Global Change Biology*, 29, 702–718,
636 <https://doi.org/10.1111/gcb.16495>, 2023.
- 637 McDermid, S., Nocco, M., Lawston-Parker, P., Keune, J., Pokhrel, Y., Jain, M.,
638 Jägermeyr, J., Brocca, L., Massari, C., Jones, A. D., Vahmani, P., Thiery, W., Yao, Y.,
639 Bell, A., Chen, L., Dorigo, W., Hanasaki, N., Jasechko, S., Lo, M.-H., Mahmood, R.,
640 Mishra, V., Mueller, N. D., Niyogi, D., Rabin, S. S., Sloat, L., Wada, Y., Zappa, L., Chen,
641 F., Cook, B. I., Kim, H., Lombardozzi, D., Polcher, J., Ryu, D., Santanello, J., Satoh,
642 Y., Seneviratne, S., Singh, D., and Yokohata, T.: Irrigation in the Earth system, *Nat Rev*
643 *Earth Environ*, <https://doi.org/10.1038/s43017-023-00438-5>, 2023.
- 644 Munia, H., Guillaume, J. H. A., Mirumachi, N., Porkka, M., Wada, Y., and Kummu,
645 M.: Water stress in global transboundary river basins: significance of upstream water
646 use on downstream stress, *Environ. Res. Lett.*, 11, 014002,
647 <https://doi.org/10.1088/1748-9326/11/1/014002>, 2016.
- 648 O'Connor, J. C., Dekker, S. C., Staal, A., Tuinenburg, O. A., Rebel, K. T., and
649 Santos, M. J.: Forests buffer against variations in precipitation, *Global Change Biology*,
650 27, 4686–4696, <https://doi.org/10.1111/gcb.15763>, 2021.
- 651 Pissarra, T. C. T., Sanches Fernandes, L. F., and Pacheco, F. A. L.: Production of
652 clean water in agriculture headwater catchments: A model based on the payment for
653 environmental services, *Science of The Total Environment*, 785, 147331,
654 <https://doi.org/10.1016/j.scitotenv.2021.147331>, 2021.
- 655 Pranindita, A., Wang-Erlandsson, L., Fetzer, I., and Teuling, A. J.: Moisture
656 recycling and the potential role of forests as moisture source during European
657 heatwaves, *Clim Dyn*, 58, 609–624, <https://doi.org/10.1007/s00382-021-05921-7>, 2022.
- 658 Qin, Y.: Global competing water uses for food and energy, *Environ. Res. Lett.*, 16,
659 064091, <https://doi.org/10.1088/1748-9326/ac06fa>, 2021.
- 660 Rockström, J., Mazzucato, M., Andersen, L. S., Fahrländer, S. F., and Gerten, D.:
661 Why we need a new economics of water as a common good, *Nature*, 615, 794–797,
662 <https://doi.org/10.1038/d41586-023-00800-z>, 2023.
- 663 Schyns, J. F., Hoekstra, A. Y., Booij, M. J., Hogeboom, R. J., and Mekonnen, M.
664 M.: Limits to the world's green water resources for food, feed, fiber, timber, and
665 bioenergy, *Proceedings of the National Academy of Sciences*, 116, 4893–4898,
666 <https://doi.org/10.1073/pnas.1817380116>, 2019.
- 667 Shao, R., Zhang, B., Su, T., Long, B., Cheng, L., Xue, Y., and Yang, W.: Estimating
668 the Increase in Regional Evaporative Water Consumption as a Result of Vegetation
669 Restoration Over the Loess Plateau, China, *Journal of Geophysical Research:*
670 *Atmospheres*, 124, 11783–11802, <https://doi.org/10.1029/2019JD031295>, 2019.
- 671 Sheng, J. and Webber, M.: Incentive coordination for transboundary water
672 pollution control: The case of the middle route of China's South-North water Transfer
673 Project, *Journal of Hydrology*, 598, 125705,
674 <https://doi.org/10.1016/j.jhydrol.2020.125705>, 2021.
- 675 Staal, A., Koren, G., Tejada, G., and Gatti, L. V.: Moisture origins of the Amazon
676 carbon source region, *Environ. Res. Lett.*, 18, 044027, <https://doi.org/10.1088/1748-9326/acc676>, 2023.
- 678 Su, Y., Li, X., Feng, M., Nian, Y., Huang, L., Xie, T., Zhang, K., Chen, F., Huang,
679 W., Chen, J., and Chen, F.: High agricultural water consumption led to the continued

- 680 shrinkage of the Aral Sea during 1992–2015, *Science of The Total Environment*, 777,
681 145993, <https://doi.org/10.1016/j.scitotenv.2021.145993>, 2021.
- 682 Sun, G., Zhou, G., Zhang, Z., Wei, X., McNulty, S. G., and Vose, J. M.: Potential
683 water yield reduction due to forestation across China, *Journal of Hydrology*, 328, 548–
684 558, <https://doi.org/10.1016/j.jhydrol.2005.12.013>, 2006.
- 685 Sun, Y., Clemens, S. C., Morrill, C., Lin, X., Wang, X., and An, Z.: Influence of
686 Atlantic meridional overturning circulation on the East Asian winter monsoon, *Nature*
687 *Geosci*, 5, 46–49, <https://doi.org/10.1038/ngeo1326>, 2012.
- 688 Theeuwens, J. J. E., Staal, A., Tuinenburg, O. A., Hamelers, B. V. M., and Dekker,
689 S. C.: Local moisture recycling across the globe, *Hydrology and Earth System Sciences*,
690 27, 1457–1476, <https://doi.org/10.5194/hess-27-1457-2023>, 2023.
- 691 Tian, B. and Fan, K.: Factors favorable to frequent extreme precipitation in the
692 upper Yangtze River Valley, *Meteorol Atmos Phys*, 121, 189–197,
693 <https://doi.org/10.1007/s00703-013-0261-9>, 2013.
- 694 Tuinenburg, O. A. and Staal, A.: Tracking the global flows of atmospheric
695 moisture and associated uncertainties, *Hydrology and Earth System Sciences*, 24,
696 2419–2435, <https://doi.org/10.5194/hess-24-2419-2020>, 2020.
- 697 Tuinenburg, O. A., Theeuwens, J. J. E., and Staal, A.: High-resolution global
698 atmospheric moisture connections from evaporation to precipitation, *Earth System*
699 *Science Data*, 12, 3177–3188, <https://doi.org/10.5194/essd-12-3177-2020>, 2020.
- 700 Varis, O. and Vakkilainen, P.: China’s 8 challenges to water resources management
701 in the first quarter of the 21st Century, *Geomorphology*, 41, 93–104,
702 [https://doi.org/10.1016/S0169-555X\(01\)00107-6](https://doi.org/10.1016/S0169-555X(01)00107-6), 2001.
- 703 Veldkamp, T. I. E., Wada, Y., Aerts, J. C. J. H., Döll, P., Gosling, S. N., Liu, J.,
704 Masaki, Y., Oki, T., Ostberg, S., Pokhrel, Y., Satoh, Y., Kim, H., and Ward, P. J.: Water
705 scarcity hotspots travel downstream due to human interventions in the 20th and 21st
706 century, *Nat Commun*, 8, 15697, <https://doi.org/10.1038/ncomms15697>, 2017.
- 707 Viviroli, D., Kummu, M., Meybeck, M., Kallio, M., and Wada, Y.: Increasing
708 dependence of lowland populations on mountain water resources, *Nat Sustain*, 3, 917–
709 928, <https://doi.org/10.1038/s41893-020-0559-9>, 2020.
- 710 Wang, S., Fu, B., Liang, W., Liu, Y., and Wang, Y.: Driving forces of changes in
711 the water and sediment relationship in the Yellow River, *Science of The Total*
712 *Environment*, 576, 453–461, <https://doi.org/10.1016/j.scitotenv.2016.10.124>, 2017.
- 713 Wang, X., Zhang, Z., Zhang, B., Tian, L., Tian, J., Arnault, J., Kunstmann, H., and
714 He, C.: Quantifying the Impact of Land Use and Land Cover Change on Moisture
715 Recycling With Convection-Permitting WRF-Tagging Modeling in the Agro-Pastoral
716 Ecotone of Northern China, *Journal of Geophysical Research: Atmospheres*, 128,
717 e2022JD038421, <https://doi.org/10.1029/2022JD038421>, 2023a.
- 718 Wang, Y., Liu, X., Zhang, D., and Bai, P.: Tracking Moisture Sources of
719 Precipitation Over China, *Journal of Geophysical Research: Atmospheres*, 128,
720 e2023JD039106, <https://doi.org/10.1029/2023JD039106>, 2023b.
- 721 Wang-Erlandsson, L., Fetzer, I., Keys, P. W., van der Ent, R. J., Savenije, H. H. G.,
722 and Gordon, L. J.: Remote land use impacts on river flows through atmospheric
723 teleconnections, *Hydrology and Earth System Sciences*, 22, 4311–4328,
724 <https://doi.org/10.5194/hess-22-4311-2018>, 2018.

- 725 Wang-Erlandsson, L., Tobian, A., van der Ent, R. J., Fetzer, I., te Wierik, S., Porkka,
726 M., Staal, A., Jaramillo, F., Dahlmann, H., Singh, C., Greve, P., Gerten, D., Keys, P. W.,
727 Gleeson, T., Cornell, S. E., Steffen, W., Bai, X., and Rockström, J.: A planetary
728 boundary for green water, *Nat Rev Earth Environ*, 3, 380–392,
729 <https://doi.org/10.1038/s43017-022-00287-8>, 2022.
- 730 Wei, F., Wang, S., Fu, B., Li, Y., Huang, Y., Zhang, W., and Fensholt, R.:
731 Quantifying the precipitation supply of China’s drylands through moisture recycling,
732 *Agricultural and Forest Meteorology*, 352, 110034,
733 <https://doi.org/10.1016/j.agrformet.2024.110034>, 2024.
- 734 Weng, W., Luedeke, M. K. B., Zemp, D. C., Lakes, T., and Kropp, J. P.: Aerial and
735 surface rivers: downwind impacts on water availability from land use changes in
736 Amazonia, *Hydrology and Earth System Sciences*, 22, 911–927,
737 <https://doi.org/10.5194/hess-22-911-2018>, 2018.
- 738 te Wierik, S. A., Cammeraat, E. L. H., Gupta, J., and Artzy-Randrup, Y. A.:
739 Reviewing the Impact of Land Use and Land-Use Change on Moisture Recycling and
740 Precipitation Patterns, *Water Resources Research*, 57, e2020WR029234,
741 <https://doi.org/10.1029/2020WR029234>, 2021.
- 742 Wu, B. and Wang, J.: Winter Arctic Oscillation, Siberian High and East Asian
743 Winter Monsoon, *Geophysical Research Letters*, 29, 3-1-3-4,
744 <https://doi.org/10.1029/2002GL015373>, 2002.
- 745 Xie, D., Zhang, Y., Zhang, M., Tian, Y., Cao, Y., Mei, Y., Liu, S., and Zhong, D.:
746 Hydrological impacts of vegetation cover change in China through terrestrial moisture
747 recycling, *Science of The Total Environment*, 915, 170015,
748 <https://doi.org/10.1016/j.scitotenv.2024.170015>, 2024.
- 749 Ya-Feng, Z., Min, D., Ya-Jing, L., and Yao, R.: Evolution characteristics and policy
750 implications of new urbanization in provincial capital cities in Western China, *PLoS*
751 *ONE*, 15, e0233555, <https://doi.org/10.1371/journal.pone.0233555>, 2020.
- 752 Yang, Z., Qian, Y., Liu, Y., Berg, L. K., Hu, H., Dominguez, F., Yang, B., Feng, Z.,
753 Gustafson Jr, W. I., Huang, M., and Tang, Q.: Irrigation Impact on Water and Energy
754 Cycle During Dry Years Over the United States Using Convection-Permitting WRF and
755 a Dynamical Recycling Model, *Journal of Geophysical Research: Atmospheres*, 124,
756 11220–11241, <https://doi.org/10.1029/2019JD030524>, 2019.
- 757 Zemp, D. C., Schleussner, C.-F., Barbosa, H. M. J., van der Ent, R. J., Donges, J.
758 F., Heinke, J., Sampaio, G., and Rammig, A.: On the importance of cascading moisture
759 recycling in South America, *Atmospheric Chemistry and Physics*, 14, 13337–13359,
760 <https://doi.org/10.5194/acp-14-13337-2014>, 2014.
- 761 Zhang, B., Tian, L., Zhao, X., and Wu, P.: Feedbacks between vegetation
762 restoration and local precipitation over the Loess Plateau in China, *Sci. China Earth*
763 *Sci.*, 64, 920–931, <https://doi.org/10.1007/s11430-020-9751-8>, 2021.
- 764 Zhang, B., Gao, H., and Wei, J.: Identifying potential hotspots for atmospheric
765 water resource management and source-sink analysis, *CSB*, 68, 2678–2689,
766 <https://doi.org/10.1360/TB-2022-1275>, 2023a.
- 767 Zhang, C., Chen, D., Tang, Q., and Huang, J.: Fate and Changes in Moisture
768 Evaporated From the Tibetan Plateau (2000–2020), *Water Resources Research*, 59,
769 e2022WR034165, <https://doi.org/10.1029/2022WR034165>, 2023b.
- 770 Zhang, C., Zhang, X., Tang, Q., Chen, D., Huang, J., Wu, S., and Liu, Y.:

771 Quantifying precipitation moisture contributed by different atmospheric circulations
 772 across the Tibetan Plateau, *Journal of Hydrology*, 628, 130517,
 773 <https://doi.org/10.1016/j.jhydrol.2023.130517>, 2024.

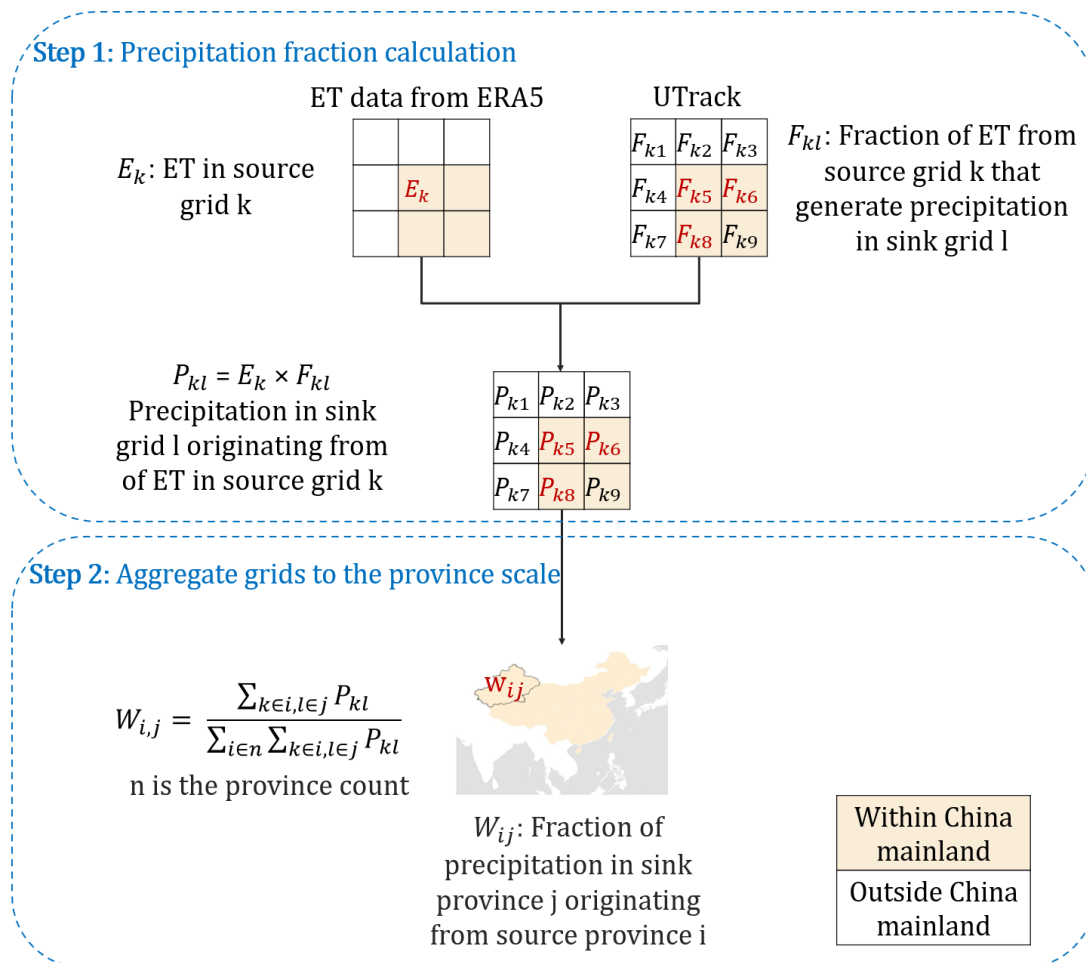
774 Zhao, Y. and Zhou, T.: Interannual Variability of Precipitation Recycle Ratio Over
 775 the Tibetan Plateau, *Journal of Geophysical Research: Atmospheres*, 126,
 776 e2020JD033733, <https://doi.org/10.1029/2020JD033733>, 2021.

777 Zhou, G., Wei, X., Chen, X., Zhou, P., Liu, X., Xiao, Y., Sun, G., Scott, D. F., Zhou,
 778 S., Han, L., and Su, Y.: Global pattern for the effect of climate and land cover on water
 779 yield, *Nat Commun*, 6, 5918, <https://doi.org/10.1038/ncomms6918>, 2015a.

780 Zhou, Y., Huang, H. Q., Nanson, G. C., Huang, C., and Liu, G.: Progradation of
 781 the Yellow (Huanghe) River delta in response to the implementation of a basin-scale
 782 water regulation program, *Geomorphology*, 243, 65–74,
 783 <https://doi.org/10.1016/j.geomorph.2015.04.023>, 2015b.

784

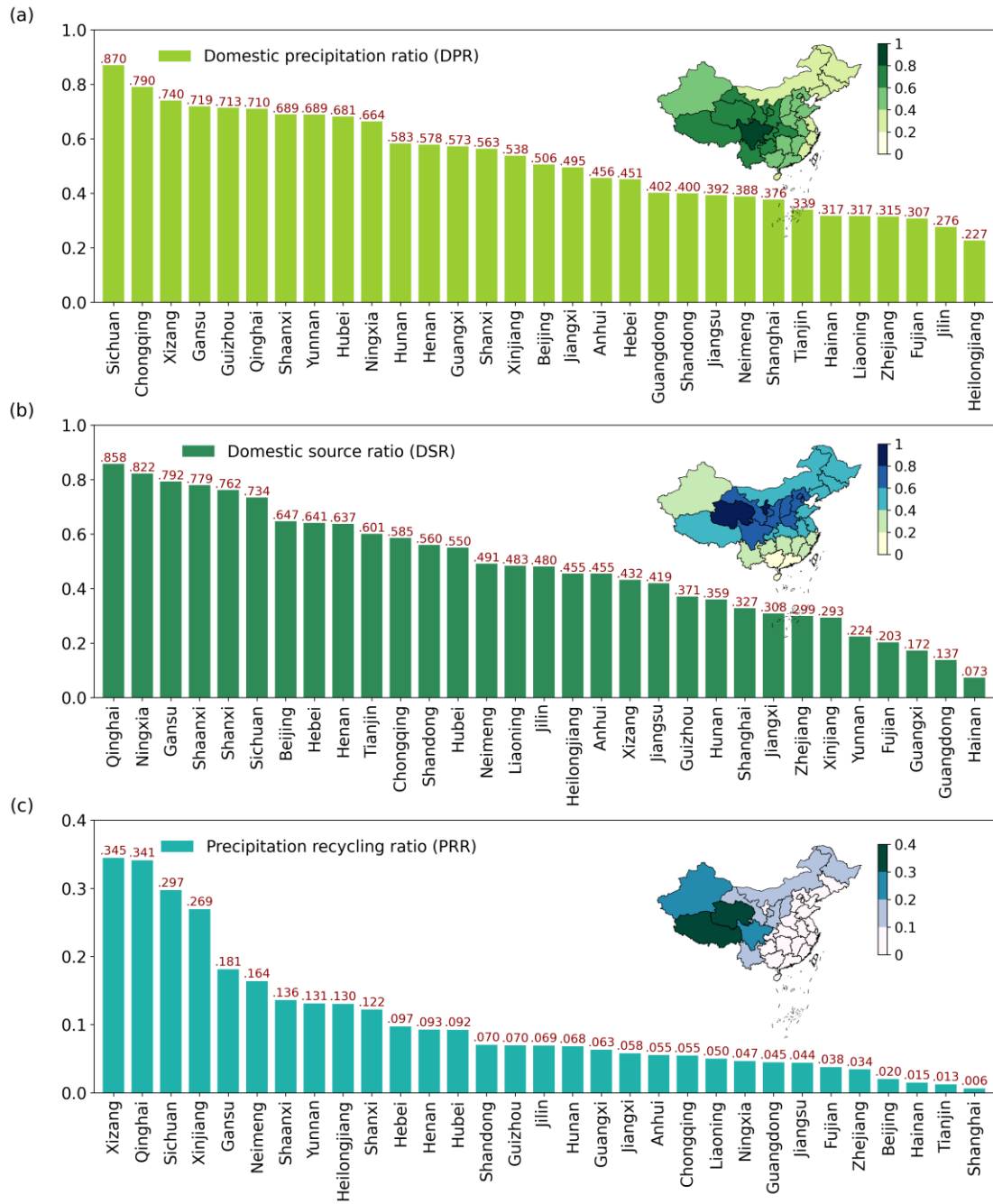
785 **Appendix A**



786

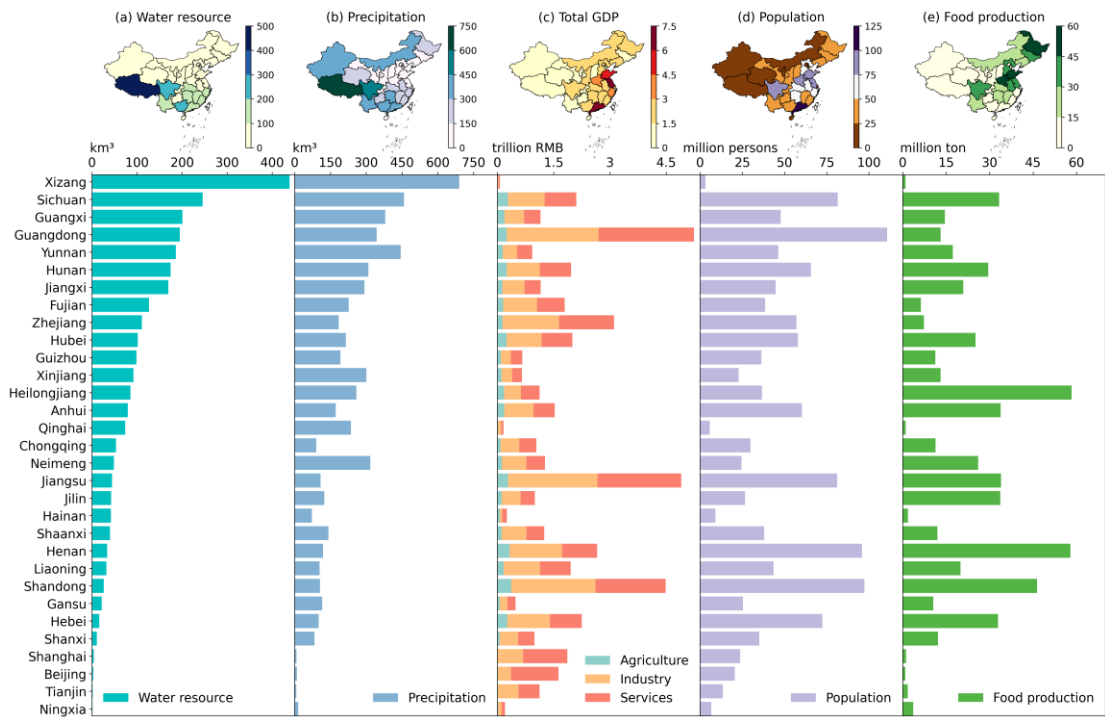
787 **Figure A1.** Workflow of estimating green water flow. Step 1: calculate the precipitation in sink
 788 grids originating from ET in source grids. Step 2: calculate the fraction of precipitation in sink
 789 provinces originating from source provinces.

790



791
792
793
794

Figure A2. (a) Domestic precipitation ratio (DPR), (b) domestic source ratio (DSR) and (c) precipitation recycling ratio (PRR) in each province.



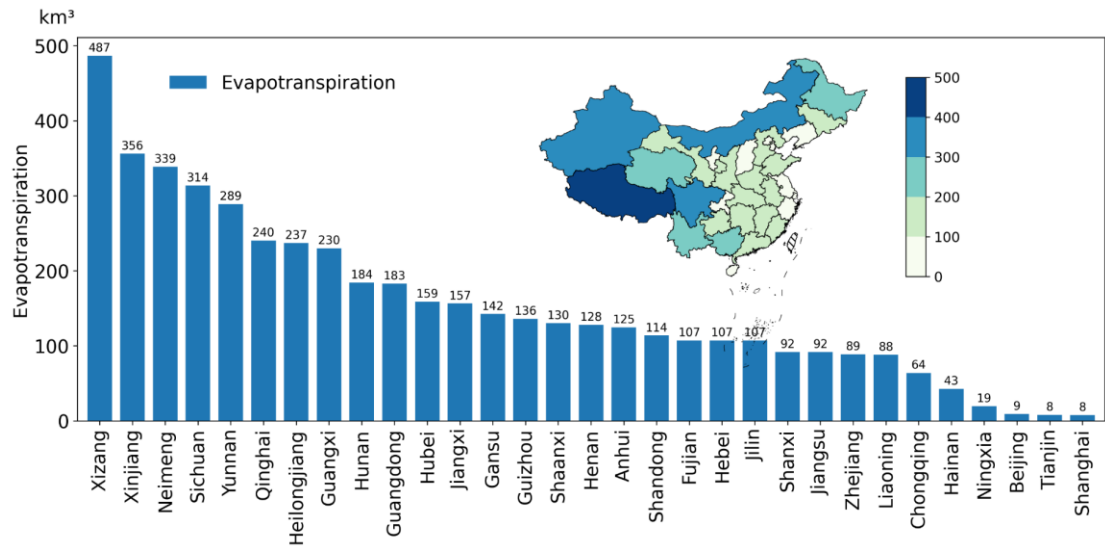
795

796

797

798

Figure A3. Water resource (a), precipitation (b), GDP (c), population (d) and food production (e) in each province.

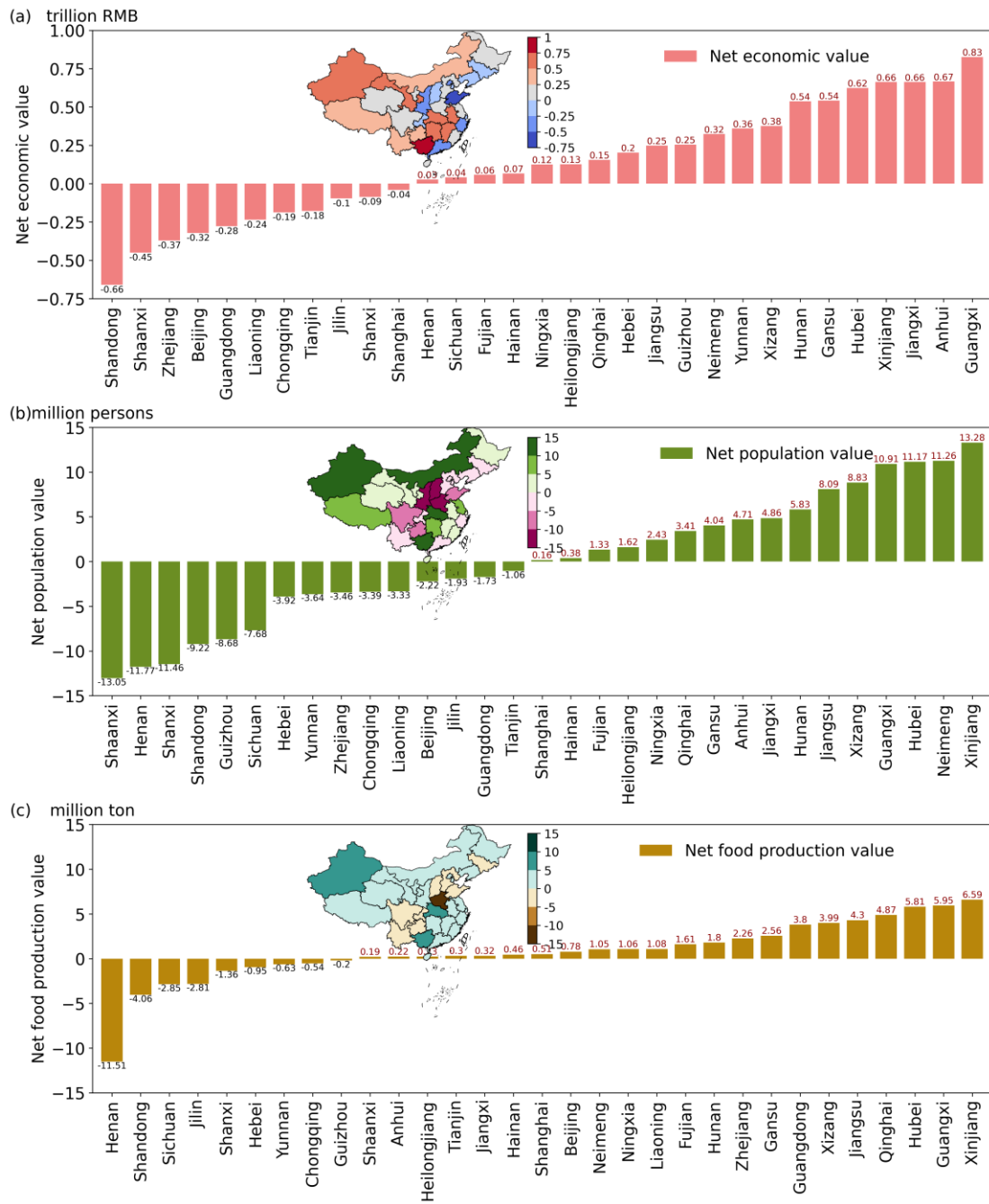


799

800

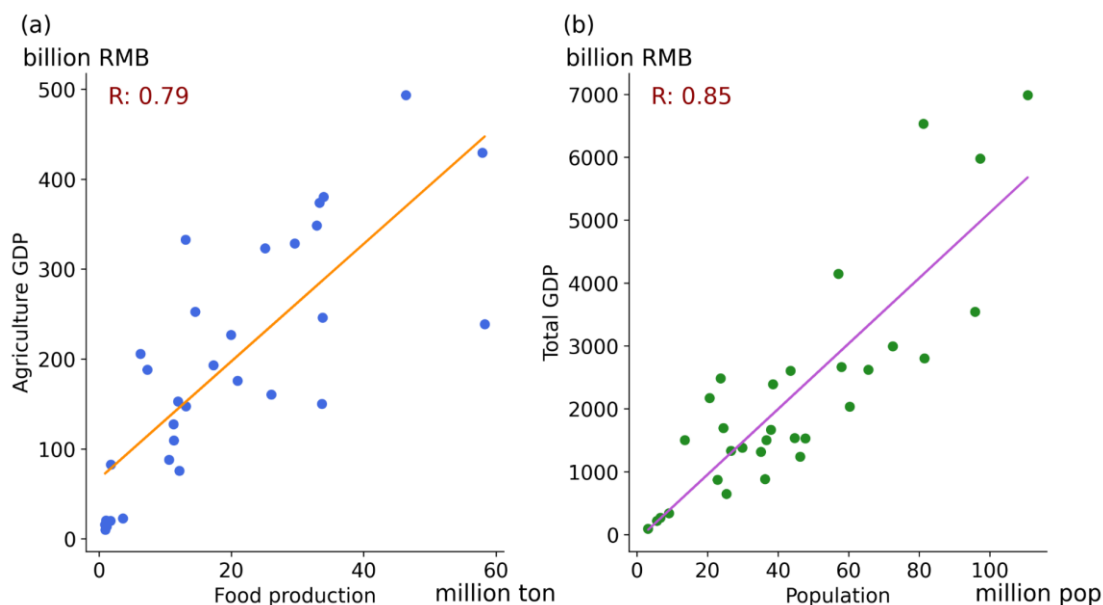
801

Figure A4. Mean evapotranspiration of 2008 to 2017 in each province.



802
803
804
805
806
807
808

Figure A5. Net ~~economic output~~GDP (a), population (b), food production (c) value of green water flow in each source province. Negative to sink provinces. Positive values represent these socio-economic values of water resource formed by green water increase by flowing from source to sink provinces. PositiveNegative values represent these socio-economic values of water resource formed by green water decrease by flowing.



809

810 **Figure A6.** Spatial pearson correlation coefficient between agricultural GDP and food production
 811 (a), population and total GDP (b) across provinces in China.

812

813 **Table A1.** Precipitation, water resources, and the contribution from green water in provinces of
 814 China.

Province	Local precipitation (km ³)	Precipitation formed by green water (km ³)	Percentage of precipitation contribution to local precipitation (%)	Local water resource (km ³)	Water resource formed by green water (km ³)	Percentage of water resource contribution to local water resource (%)
Beijing	9.47	4.53	48	2.82	1.14	40
Tianjin	7.12	2.66	37	1.62	0.70	43
Hebei	100.50	48.35	48	15.98	12.26	77
Shanxi	82.88	51.69	62	10.91	12.38	113
Neimeng	317.11	131.57	41	48.79	31.80	65
Liaoning	104.53	27.80	27	31.92	8.40	26
Jilin	124.15	29.55	24	42.21	8.98	21
Heilongjiang	258.88	53.75	21	85.40	15.44	18
Shanghai	8.02	2.83	35	4.04	1.19	29
Jiangsu	108.09	35.93	33	44.27	13.43	30
Zhejiang	184.72	27.98	15	110.66	13.46	12
Anhui	172.36	56.84	33	79.67	23.19	29
Fujian	226.74	32.96	15	126.39	17.33	14
Jiangxi	292.56	77.52	26	169.44	39.25	23
Shandong	105.99	45.49	43	25.99	13.56	52
Henan	118.83	73.87	62	33.73	24.08	71
Hubei	214.46	108.13	50	101.66	45.27	45

Hunan	308.87	107.25	35	174.33	52.28	30
Guangdong	344.05	73.31	21	194.77	38.54	20
Guangxi	379.82	131.63	35	200.76	66.32	33
Hainan	72.47	13.50	19	41.86	7.13	17
Chongqing	90.61	50.45	56	53.23	21.87	41
Sichuan	458.97	272.93	59	245.86	124.43	51
Guizhou	191.84	97.05	51	98.49	46.54	47
Yunnan	444.68	199.06	45	185.99	96.34	52
Xizang	689.68	360.21	52	438.59	200.33	46
Shaanxi	141.21	89.70	64	39.82	26.14	66
Gansu	115.45	102.36	89	21.60	30.31	140
Qinghai	236.12	170.62	72	73.50	63.57	86
Ningxia	14.95	12.94	87	0.98	3.34	342
Xinjiang	300.10	191.37	64	91.95	64.92	71
Total	6225.19	2683.84	43	2.82	1.14	40

815

816 **Table A2.** The embodied socio-economic values of green water flow from source
817 provinces for water resources, GDP by industry, population, and food production.

818 Socio-economic indicators are the average value of 2008-2017.

Province	Total GDP (Trillion CNY)	Agriculture GDP (Trillion CNY)	Industry GDP (Trillion CNY)	Service GDP (Trillion CNY)	Population (Million persons)	Food production (Million ton)
Beijing	0.13	0.01	0.05	0.07	2.05	0.97
Tianjin	0.09	0.01	0.04	0.04	1.33	0.61
Hebei	1.27	0.09	0.56	0.62	22	10.82
Shanxi	1.18	0.09	0.54	0.55	22.36	10.35
Neimeng	1.67	0.15	0.77	0.75	30.77	21.78
Liaoning	0.40	0.04	0.19	0.17	7.23	5.92
Jilin	0.27	0.03	0.12	0.11	5.34	6.37
Heilongjiang	0.39	0.05	0.17	0.17	8.04	10.45
Shanghai	0.09	0.01	0.04	0.04	1.41	0.57
Jiangsu	1.06	0.08	0.51	0.47	18.13	8.5
Zhejiang	0.69	0.04	0.32	0.32	11.08	4.11
Anhui	1.37	0.11	0.66	0.59	25.42	11.85
Fujian	0.56	0.04	0.27	0.26	9.46	2.93
Jiangxi	1.33	0.10	0.64	0.59	24.34	9.43
Shandong	1.37	0.11	0.65	0.62	23.85	11.72
Henan	1.75	0.15	0.85	0.75	34.94	16.74
Hubei	1.98	0.18	0.96	0.84	40.57	18.56
Hunan	1.63	0.15	0.78	0.70	33.2	14.13

Guangdong	1.10	0.08	0.52	0.49	20.09	6.38
Guangxi	1.54	0.14	0.73	0.67	33.06	12.7
Hainan	0.18	0.01	0.08	0.08	3.42	1.05
Chongqing	0.66	0.06	0.32	0.28	14.92	6.4
Sichuan	2.31	0.25	1.10	0.96	58.39	24.16
Guizhou	1.08	0.11	0.51	0.46	25.05	10.25
Yunnan	1.48	0.16	0.69	0.63	38.21	14.98
Xizang	0.56	0.07	0.26	0.23	15.32	5.97
Shaanxi	1.48	0.13	0.71	0.64	30.87	14
Gansu	1.05	0.10	0.50	0.46	24.22	10.96
Qinghai	0.72	0.07	0.34	0.31	18.3	7.56
Ningxia	0.18	0.02	0.09	0.08	3.88	1.85
Xinjiang	1.00	0.11	0.46	0.43	22.03	11.6
Total (percentage of total contribution to local socio-economic value)	30.56 (45%)	2.74 (46%)	14.43 (45%)	13.39 (44%)	629.28 (46%)	293.67 (50%)

819